

Nanodiamonds carrying silicon-vacancy quantum emitters with almost lifetime-limited linewidths

Uwe Jantzen¹, Andrea B Filipovski (Kurz)^{1,‡},
 Daniel S Rudnicki², Clemens Schäfermeier³, Kay D Jahnke¹,
 Ulrik L Andersen³, Valery A Davydov⁴,
 Viatcheslav N Agafonov⁵, Alexander Kubanek¹,
 Lachlan J Rogers¹, Fedor Jelezko¹

¹ Institute for Quantum Optics and Integrated Quantum Science and Technology (IQst), Ulm University, Albert-Einstein-Allee 11, D-89081 Ulm, Germany

² Institute of Physics, Jagiellonian University, Lojasiewicza 11, 30-348 Krakow, Poland

³ Technical University of Denmark, Department of Physics, 2800 Kongens Lyngby, Denmark

⁴ L.F. Vereshchagin Institute for High Pressure Physics, Russian Academy of Sciences, Troitsk, Moscow, 142190 Russia

⁵ GREMAN, UMR CNRS CEA 6157, Université F. Rabelais, 37200 Tours, France

E-mail: lachlan.j.rogers@quantum.diamonds

Abstract. Colour centres in nanodiamonds are an important resource for applications in quantum sensing, biological imaging, and quantum optics. Here we report unprecedented narrow optical transitions for individual colour centres in nanodiamonds smaller than 200 nm. This demonstration has been achieved using the negatively-charged silicon vacancy centre, which has recently received considerable attention due to its superb optical properties in bulk diamond. We have measured an ensemble of silicon-vacancy centres across numerous nanodiamonds to have an inhomogeneous distribution of 1.05 nm at 5 K. Individual spectral lines as narrower than 360 MHz were measured in photoluminescence excitation, and correcting for apparent spectral diffusion yielded an homogeneous linewidth of about 200 MHz which is close to the lifetime limit. These results indicate the high crystalline quality achieved in these nanodiamond samples, and advance the applicability of nanodiamond-hosted colour centres for quantum optics applications.

Submitted to: *New J. Phys.*

‡ This author has changed their name since the original version was posted on arXiv.org.

Nanodiamonds (NDs) hosting optically active point defects (“colour centres”) are an important technical material for applications in quantum sensing [1], biological imaging [2–4], and quantum optics [5]. One colour centre which has attracted recent attention is the negatively charged silicon vacancy (SiV^-) defect, which consists of a silicon atom taking the place of two adjacent carbon atoms in the lattice [6]. The SiV^- centre in diamond has risen to prominence on the basis of its superb spectral properties, including a strong zero-phonon line (ZPL) at 737 nm which contains 70% of the fluorescence from this colour centre [7]. In low-strain bulk diamond, the SiV^- centre has exhibited lifetime-limited spectral linewidths at 4K with no spectral diffusion [8]. These ideal properties have enabled the efficient production of indistinguishable photons from distinct emitters [9]. Recent studies in bulk diamond have shown that the electronic spin coherence time in the SiV^- centre is fundamentally limited by fast phonon-induced orbital relaxation in the ground state [10, 11]. Small NDs should impose boundary conditions that prevent the availability of phonons at the critical frequency, thereby extending coherence time. This has increased the motivation to find well-behaved SiV^- centres in the nanodiamond environment.

Although SiV^- centres have been observed to fluoresce in NDs as small as molecules (1.6 nm) [12], the ND host has always led to less homogeneous photon emission [13–16]. Some promising results have been recently reported for larger hybrid nanostructures [17], but the obstacle persists for SiV^- applications requiring ND environments. Here we report unprecedented optical properties of SiV^- colour centres hosted in nanodiamonds. Individual spectral lines close to the lifetime limit were measured for SiV^- centres in nanodiamonds smaller than 200 nm, representing an improvement of nearly four times over the best SiV^- line previously reported for nanodiamonds [18]. Such narrow lines in small nanodiamonds are of interest for a range of applications, including coupling to cavities [19].

The nanodiamond crystals used in this study were produced using a recently reported synthesis technique [20]. This novel technique directly produces nanometre- and micrometre-sized crystals during high-pressure high-temperature (HPHT) diamond synthesis. HPHT diamond synthesis reproduces the conditions required for natural diamond formation, where the pressure and temperature make diamond the stable form of carbon. In contrast to industrial bulk diamond synthesis, the metal catalyst was left out in order to ensure micro- and nanodiamond growth. Silicon was introduced during the growth process, and incorporated into the diamond crystals to form the negatively-charged silicon vacancy centre. The narrow spectral lines reported here demonstrate that this direct HPHT synthesis technique is capable of producing nanodiamonds with high crystalline quality, which are therefore a valuable technical material for quantum optics applications.

The nanodiamonds were suspended in a solution of ultrapure water and ethanol, and were ultrasonicated to disperse the crystals. This solution was spin coated on a thermally conducting substrate (type IIa diamond) containing markers to facilitate accurate comparison between confocal fluorescence imaging and scanning electron

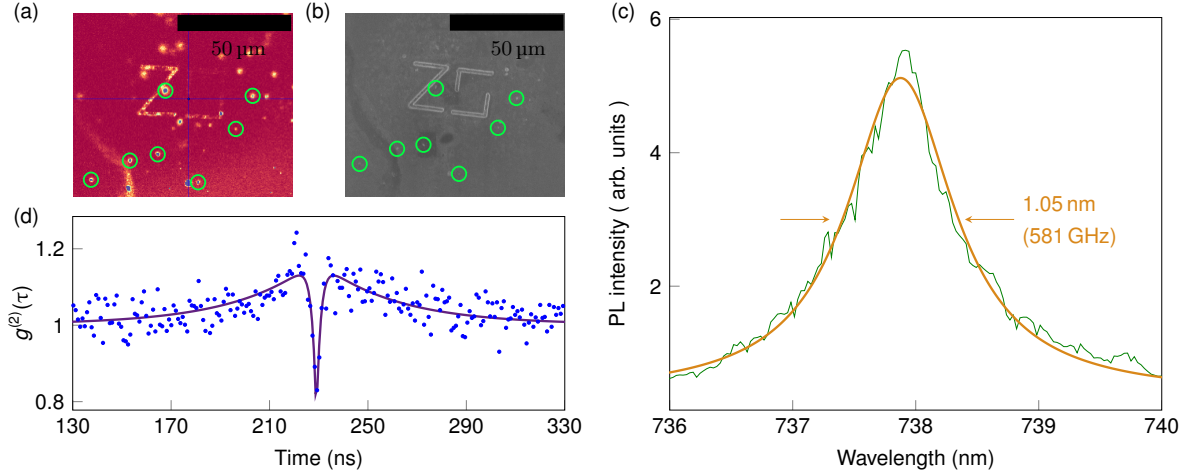


Figure 1. Spectral distribution across multiple nanodiamonds. (a) Fluorescence image of NDs on a diamond substrate near a marker. Green circles mark spots containing SiV⁻ centres as identified by their fluorescence spectrum. (b) SEM image of same sample region. The marked spots were identified as NDs (or clusters of NDs) in the SEM and their size determined with an accuracy of 20 nm. (c) Photoluminescence spectrum averaged over 7 fluorescent spots containing a total of more than 50 SiV⁻ centres. The illustrated lorentzian fit was used to measure the linewidth. (d) The most visible dip in the $g^{(2)}$ function at a fluorescence spot was only to a depth of 82 %, corresponding to about 6 emitters (assuming equal brightness).

microscope (SEM) imaging, as shown in Figure 1(a) and (b). This enabled correlation of the optical spectroscopy with the ND shape and size. Optical excitation was provided by a continuous-wave 532 nm frequency-doubled diode-pumped solid-state laser. Fluorescence images and spectra were recorded with a home-built confocal microscope, using an air objective with NA=0.95. To resolve the fine-structure of the SiV⁻ the sample was mounted in a helium-flow-cryostat. The cryostat cold-finger reached a temperature of 5 K, and the thermal conductivity of the substrate suggested that the NDs were at a temperature below 8 K. Photoluminescence spectra were measured on a spectrometer (grating with 1200 lines/mm) for 7 fluorescent spots containing several SiV⁻ centres. The summed ensemble zero-phonon line is shown in Figure 1(c), and was found to have a linewidth of 1.05 nm (581 GHz) representing the inhomogeneous distribution across multiple SiV⁻ centres. This is broader than SiV⁻ ensembles in low-strain bulk diamond which exhibited linewidths of 8 GHz [21], but narrower than previously reported ND observations of about 5 nm (3 THz) [22]. It is concluded that the novel HPHT fabrication technique used here is capable of producing NDs with a more uniform crystal lattice than previous fabrication methods.

Due to the diffraction limited resolution of optical microscopy, bright spots in the fluorescence image did not necessarily correspond to individual SiV⁻ centres or even to individual nanodiamonds. Photon autocorrelation statistics (the $g^{(2)}$ function) are typically used to demonstrate single-emitter detection (where $g^{(2)}(0) < 0.5$). The deepest dip observed here was only to a relative height of $g^{(2)}(0) = 0.82$ as shown in

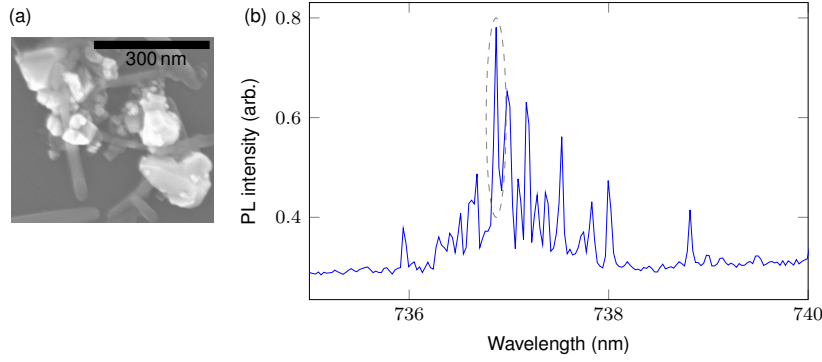


Figure 2. PL for a single spot in the confocal image. (a) SEM image showing this spot is made up of a number of NDs each smaller than 200 nm. It was not possible to associate spectral features with specific NDs within the cluster. (b) PL spectrum recorded for this ND cluster, showing many lines corresponding to numerous SiV⁻ centres. The circled line is the location of the feature examined in PLE in Figure 3.

Figure 1(d). This corresponds to six emitters if they were equally bright, and more than six if some were lying outside the optimum collection region of the confocal microscope. Most of the fluorescent spots did not produce a measurable dip, suggesting the presence of many SiV⁻ centres.

Despite the ultrasonication used in sample preparation, SEM imaging revealed clustering of NDs as shown in Figure 2(a), resulting in more than one ND in the confocal detection spot. In this case it was not possible to determine which of the clustered NDs contained SiV⁻ centres. Subsequent to the measurements reported here, some nanodiamonds were spin-coated from a solution of chloroform (with residual ethanol and ultrapure water) following comments in [28], and this reduced clustering but did not eliminate it. Future experiments may be able to further reduce the clustering of NDs through more advanced preparation techniques. The PL spectra that exhibited a SiV⁻ ZPL were typically found to contain more than the four-line structure that is expected for a single centre [6, 23, 24], as shown in Figure 2(b). This is another indication of the presence of multiple SiV⁻ centres in the fluorescence detection volume. From the $g^{(2)}$ data and clustering observations we conclude that the inhomogeneous linewidth in Figure 1(c) is from an ensemble of more than 50 SiV⁻ centres. An interesting implication of the high number-density of SiV⁻ in these small NDs is the reasonable probability of two centres being in close proximity. For two nearly resonant centres at close separation, direct dipole-dipole interaction would cause a shifting of the spectral lines. It is possible that this effect contributes to a broadening of the ensemble linewidth.

Since spatial resolution was unable to isolate individual SiV⁻ centres, resonant excitation techniques were used to allow spectral isolation. To perform photoluminescence excitation (PLE) spectroscopy a resonant laser was scanned through the zero-phonon line while fluorescence was detected off-resonantly in the 750–810 nm band (the phonon sideband). Individual isolated optical transitions were excited in this manner and the spectral linewidths were measured to high precision (the instrument

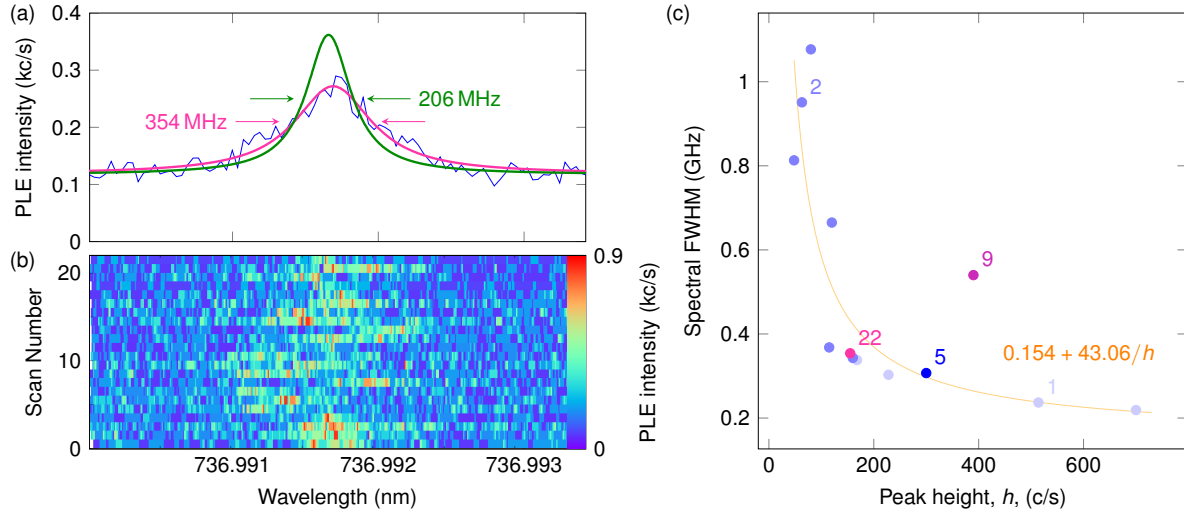


Figure 3. Resonant excitation to probe individual SiV⁻-centres. (a) Photoluminescence excitation (PLE) spectrum of a single transition with averaged linewidth of 354 MHz (Data in blue, fit to average in purple, spectral diffusion interpretation in green). (b) The raw data consisted of 22 separate scans, and the line position was found to vary between scans. Interpreting this as spectral diffusion and shifting each scan for correction gave a homogeneous linewidth of 206 MHz (green curve in (b)), which is close to the lifetime limit. (c) Summary of PLE measurements for 13 spectral lines, showing many with linewidths below 400 MHz. Pale blue data points are from single-pass scans of the line; middle-blue are from double-pass scans; blue, purple, magenta indicate 5, 9, 22 passes respectively. The magenta point corresponds to the data shown in (a) and (b). The distribution of points closely follows a reciprocal relationship (orange fit excludes the purple spot with 9 passes), indicating that the area under the PLE line was similar for all of these spectra. It is interpreted that some spots have spectral diffusion over about 1 GHz at a rate much faster than the measurement (broadening and lowering the PLE peak).

limit of the laser was < 100 kHz). Resonant excitation can lead to power broadening, although this effect was found to be negligible for excitation laser powers below 4 nW entering the microscope objective. Figure 3(a) shows a PLE spectrum exhibiting a SiV⁻ linewidth of 354 MHz, for a ND below 200 nm in size from the cluster shown in Figure 2(a). This is considerably narrower than the previous best SiV⁻ lines in NDs of 1.4 GHz [18].

This excitation line was measured by making multiple scans at 400 MHz/s and averaging, and it is apparent in Figure 3(b) that additional information is contained in the individual scans. The line position was observed to change with time in a manner similar to the spectral diffusion that has been observed for other colour centres in diamond [25]. Interpreting this behaviour as spectral diffusion and displacing each scan to overlap the peak positions yielded an homogeneous linewidth of 206 MHz as illustrated in Figure 3(b). The slope of the $g^{(2)}$ dip in Figure 1(d) indicates that the SiV⁻ centres in these NDs had an excited state decay lifetime of about 1.7 ns, which is consistent with measurements in bulk diamond [8]. This fluorescence lifetime imposes a

fourier-transform-limited linewidth of 100 MHz. However, it was not possible to reliably identify which of the four ZPL transitions this PLE line was associated with since the distribution of ZPL positions across the ensemble of SiV⁻ centres was far greater than the fine-structure splitting. At low temperature two of these four transitions are known to be broadened due to thermalisation in the excited state [8]. It is therefore difficult in this ND situation to compare the measured linewidth to the lifetime limit in detail, however it is clear that the values are close.

Figure 3(c) shows a summary of similar PLE measurements made for 13 SiV⁻ lines, illustrating the measured linewidth and peak height. For technical reasons including spatial drift of the confocal microscope and blinking of the SiV⁻ sites (discussed below), most of the PLE spectra were recorded in far fewer than the 22 passes contained in Figure 3(b). It is apparent that single-pass spectra typically gave a narrower linewidth than averages over multiple passes, as expected in the presence of slow spectral diffusion. However, it is striking that the peaks with the lowest amplitude also had the broadest linewidth. This is the inverse of the trend expected for the situation of power broadening. Indeed, the reciprocal relationship illustrated in Figure 3(c) shows that these PLE lines enclosed essentially the same area and therefore the linewidth variation was not related to excitation intensity. It is interpreted that these spectra corresponded to SiV⁻ sites exhibiting spectral diffusion at a rate much faster than the 50 Hz photon-counting-bins used for these measurements. Such a situation would mean that even single- or double-pass scans would trace out the averaged “envelope” of the rapidly-shifting spectral feature, leading to broader but lower peaks. Despite this broadening of some of the lines, a clear majority had similar characteristics to the line studied in Figure 3(a) and (b).

The narrow optical transitions indicate the high crystalline quality of these NDs. These results are promising for SiV⁻ applications requiring small pieces of diamond. Unfortunately, a blinking phenomenon was observed in which the fluorescence switched between two discrete levels as shown in Figure 4(a). This behaviour is consistent with previous reports of SiV⁻ centres in NDs [26], and it introduces challenges in the development of applications involving colour centres in NDs. In order to obtain more information about the processes responsible for blinking, time series of the fluorescence rate were recorded for a few minutes at various incident laser powers in the range of 30–1000 nW. Raw measurement data are included in the supplementary data (see `blinking_time_trace` csv files, available from URL). The laser frequency was chosen to maximise the fluorescence, indicating resonance with the SiV⁻ optical transition. The switching rates (R_{on} , R_{off}) were determined from the typical durations of “on” and “off” events in these time series.

A double-threshold technique was used to identify the “on” and “off” events, since in general the switching contrast was smaller than the noise amplitude as seen in Figure 4(a). In this technique the switch-on threshold was higher than the switch-off threshold. A preliminary threshold T_i was manually chosen to start this process, shown by the dashed blue line in Figure 4(a). The mean $\overline{I_{\text{off}}}$ and standard deviation σ_{off} were

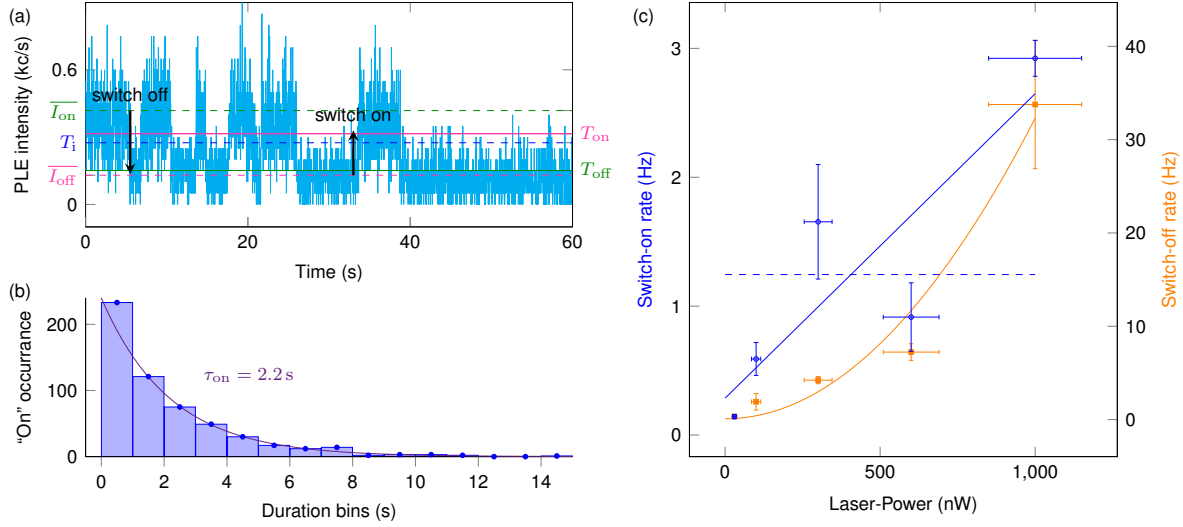


Figure 4. Blinking of fluorescence. (a) Under resonant excitation the SiV^- centres were observed to change between two discrete fluorescence levels. Here the first minute of data for 30 nW excitation power on a SiV^- line at 736.612 nm is shown as a typical example, with the switching thresholds T_{on} and T_{off} illustrated for $k = 2.5$. The raw measurement data are included in the supplementary data (see `blinking_time_trace` csv files, available from URL). (b) Histograms of duration for the “on” and “off” intervals gave exponential distributions, from which a characteristic time can be determined (and hence switching rate). The histogram for the “on” events is shown for the 30 nW data and thresholds of $k = 2.5$. (c) The “on” and “off” rates (R_{on} and R_{off}) both increase with excitation laser intensity, with linear and quadratic fits illustrated respectively. The dashed line is the best fit for a constant R_{on} . The horizontal error bars correspond to a 15% uncertainty in determining the laser power applied to the SiV^- centre, and the vertical error bars represent the uncertainty in judging a switching event.

calculated for all data points below T_i , and $\overline{T_{on}}$ and σ_{on} were determined for the data points above T_i . Actual switching thresholds were then calculated as $T_{on} = \overline{T_{off}} + k\sigma_{off}$ and $T_{off} = \overline{T_{on}} - k\sigma_{on}$ for some constant k . These thresholds mean that a switch of state is identified only if the signal deviates from the current state by more than k times the standard deviation (noise level) in the current state.

The fundamental uncertainty in extracting “on” and “off” durations from the blinking time traces arose because short switching events may be indistinguishable from noise spikes. This is directly related to the strictness of the switching thresholds T_{on} and T_{off} , which are determined by the constant k . Various thresholds beginning at $k = 2$ were used, with k increasing to the point where the threshold lost meaning (when $T_{off} < \overline{T_{off}}$, meaning that the switch-off threshold level went below the mean “off” count-rate). Because k was varied over a broad range (typically up to about $k = 3$) it was not important that the means and standard deviations arose from T_i rather than the actual T_{on} and T_{off} . For each k -value histograms were produced for the duration of on and off intervals, and characteristic time-constants were obtained from fitting the histograms with exponential decay functions as illustrated in Figure 4(b). The switching rates (R_{on} ,

R_{off}) were taken as the reciprocal of the characteristic duration of off and on intervals respectively, and are shown as a function of excitation intensity in Figure 4(c). The data points and vertical error bars in Figure 4(c) represent the mean and standard deviation of the results from the range of plausible thresholds (the range of k -values). Although the uncertainty margins are high, it is clear that both rates vary with applied laser power.

Precise identification of these switching processes is challenging and left open for further investigations, however our observations exclude a few obvious candidates. The blinking was observed using resonant excitation, which is capable of optically pumping the system to a “dark” ground state from which all excitation transitions are non-resonant. SiV^- has an orbital degeneracy in its ground state, providing a potential dark state, but if this were the cause of the blinking then the switch-on rate R_{on} would correspond to the orbital relaxation process in the ground state and should therefore be independent of excitation intensity. The best fit for such a case is illustrated in Figure 4(b) by a dashed line, and it is excluded by the data. In analogy with the nitrogen vacancy NV^-/NV^0 system, photo-ionisation would provide another potential “dark” state leading to blinking. The neutral SiV^0 centre is known in diamond, and has been attributed to a zero-phonon line at 946 nm. The 736 nm resonant excitation for SiV^- would therefore be far from resonant to SiV^0 , and is unlikely at the low intensities used here to be capable of exciting appreciable photo-ionisation back to the negative charge state. Unlike the nitrogen vacancy centre, the neutral charge state SiV^0 is too weakly fluorescent to be detectable at the single-site level, making it impossible to check for its presence in the fluorescence spectra measured here.

It has been argued that the SiV^- centre is remarkably insensitive to strain and electric field perturbations [8,9], but the shielding effects of symmetry should be reduced as the centre becomes more distorted. In nanodiamonds external charge fluctuations may well be “visible” to the SiV^- centres, and these are a plausible cause for the spectral diffusion and blinking reported here. Any surface chemistry which is photo active would account for the increasing blinking rates with higher excitation intensities. It has been shown that surface treatment can control blinking of fluorescent colour centres [27] and it is expected that future work in this direction may improve the performance of SiV^- centres in NDs. In fact, these surface effects could be the origin of both the spectral diffusion and the blinking. It was not possible to directly compare the spectral diffusion process with the observed blinking because power broadening masks the diffusion effect.

In conclusion, we have measured the narrowest SiV^- spectral lines in NDs of 354 MHz, and this can be reduced to 200 MHz after correcting for spectral diffusion. This is close to the transform limit, and suggests that these direct-HPHT synthesised NDs have a crystal quality that surpasses the NDs used in previous SiV^- experiments. This material is therefore uniquely attractive for use in quantum optics applications, including cavities. Existing limitations due to blinking effects and spectral diffusion are likely due to interaction with other defects at the surface of the NDs, and this problem is fundamental to all colour centres close to the diamond surface (regardless of crystalline

quality). This should be tackled by surface treatment.

Acknowledgements

The authors thank W. Gawlik for helpful discussions. Experiments performed for this work were operated using the Qudi software suite, available from <https://github.com/Ulm-IQO/qudi>. This work was funded from ERC project BioQ, EU projects SIQS and EQUAM, DFG (SFB/TR21 and FOR 1493), Volkswagenstiftung and BMBF. ABK and AK acknowledge support of the Carl-Zeiss Foundation. AK also acknowledges support from Wissenschaftler-Rückkehrprogramm GSO/CZS, IQST, and DFG. DR acknowledges support of the NATO 'Science for Peace' grant (CBP.MD.SFP 983932) and KNOW project. VD thanks the Russian Foundation for Basic Research (Grant No. 15-03-04490) for financial support.

Author Contributions

UJ, AF, DR, CS, KJ, and LR performed the measurements, which were conceived by LR, AK, and FJ. VD and VA supplied the nanodiamond samples. The manuscript was written by UJ, AF, and LR, and all authors discussed the results and commented on the manuscript.

References

- [1] A. Ermakova, G. Pramanik, J.-M. Cai, G. Algara-Siller, U. Kaiser, T. Weil, Y.-K. Tzeng, H. C. Chang, L. P. McGuinness, M. B. Plenio, B. Naydenov, and F. Jelezko. Detection of a Few Metallo-Protein Molecules Using Color Centers in Nanodiamonds. *Nano Letters*, 13(7):3305–3309, July 2013.
- [2] Chi-Cheng Fu, Hsu-Yang Lee, Kowa Chen, Tsong-Shin Lim, Hsiao-Yun Wu, Po-Keng Lin, Pei-Kuen Wei, Pei-Hsi Tsao, Huan-Cheng Chang, and Wunshain Fann. Characterization and application of single fluorescent nanodiamonds as cellular biomarkers. *Proceedings of the National Academy of Sciences*, 104(3):727 – 732, January 2007.
- [3] Julia Tisler, Rolf Reuter, Anke Lämmle, Fedor Jelezko, Gopalakrishnan Balasubramanian, Philip R. Hemmer, Friedemann Reinhard, and Jörg Wrachtrup. Highly Efficient FRET from a Single Nitrogen-Vacancy Center in Nanodiamonds to a Single Organic Molecule. *ACS Nano*, 5(10):7893–7898, October 2011.
- [4] David A. Simpson, Amelia J. Thompson, Mark Kowarsky, Nida F. Zeeshan, Michael S. J. Barson, Liam T. Hall, Yan Yan, Stefan Kaufmann, Brett C. Johnson, Takeshi Ohshima, Frank Caruso, Robert E. Scholten, Robert B. Saint, Michael J. Murray, and Lloyd C. L. Hollenberg. In vivo imaging and tracking of individual nanodiamonds in drosophila melanogaster embryos. *Biomedical Optics Express*, 5(4):1250–1261, April 2014.
- [5] J.-M. Le Floch, C. Bradac, N. Nand, S. Castelletto, M. E. Tobar, and T. Volz. Addressing a single spin in diamond with a macroscopic dielectric microwave cavity. *Applied Physics Letters*, 105(13):133101, September 2014.
- [6] J. P. Goss, R. Jones, S. J. Breuer, P. R. Briddon, and S. Öberg. The Twelve-Line 1.682 eV Luminescence Center in Diamond and the Vacancy-Silicon Complex. *Physical Review Letters*, 77(14):3041–3044, September 1996.

- [7] Alan T. Collins, Lars Allers, Christopher J.H. Wort, and Geoffrey A. Scarsbrook. The annealing of radiation damage in De Beers colourless CVD diamond. *Diamond and Related Materials*, 3(4–6):932–935, April 1994.
- [8] L. J. Rogers, K. D. Jahnke, T. Teraji, L. Marseglia, C. Müller, B. Naydenov, H. Schauffert, C. Kranz, J. Isoya, L. P. McGuinness, and F. Jelezko. Multiple intrinsically identical single-photon emitters in the solid state. *Nature Communications*, 5:4739, August 2014.
- [9] A. Sipahigil, K. D. Jahnke, L. J. Rogers, T. Teraji, J. Isoya, A. S. Zibrov, F. Jelezko, and M. D. Lukin. Indistinguishable Photons from Separated Silicon-Vacancy Centers in Diamond. *Physical Review Letters*, 113(11):113602, September 2014.
- [10] Lachlan J. Rogers, Kay D. Jahnke, Mathias H. Metsch, Alp Sipahigil, Jan M. Binder, Tokuyuki Teraji, Hitoshi Sumiya, Junichi Isoya, Mikhail D. Lukin, Philip Hemmer, and Fedor Jelezko. All-Optical Initialization, Readout, and Coherent Preparation of Single Silicon-Vacancy Spins in Diamond. *Physical Review Letters*, 113(26):263602, December 2014.
- [11] Kay D. Jahnke, Alp Sipahigil, Jan M. Binder, Marcus W. Doherty, Mathias Metsch, Lachlan J. Rogers, Neil B. Manson, Mikhail D. Lukin, and Fedor Jelezko. Electron-phonon processes of the silicon-vacancy centre in diamond. *New Journal of Physics*, 17(4):043011, April 2015.
- [12] Igor I. Vlasov, Andrey A. Shiryayev, Torsten Rendler, Steffen Steinert, Sang-Yun Lee, Denis Antonov, Márton Vörös, Fedor Jelezko, Anatolii V. Fisenko, Lubov F. Semjonova, Johannes Biskupek, Ute Kaiser, Oleg I. Lebedev, Ilmo Sildos, Philip R. Hemmer, Vitaly I. Konov, Adam Gali, and Jörg Wrachtrup. Molecular-sized fluorescent nanodiamonds. *Nature Nanotechnology*, 9(1):54–58, January 2014.
- [13] E. Neu, C. Arend, E. Gross, F. Guldner, C. Hepp, D. Steinmetz, E. Zscherpel, S. Ghodbane, H. Sternschulte, D. Steinmüller-Nethl, Y. Liang, A. Krueger, and C. Becher. Narrowband fluorescent nanodiamonds produced from chemical vapor deposition films. *Applied Physics Letters*, 98(24):243107–243107–3, June 2011.
- [14] Elke Neu, David Steinmetz, Janine Riedrich-Möller, Stefan Gsell, Martin Fischer, Matthias Schreck, and Christoph Becher. Single photon emission from silicon-vacancy colour centres in chemical vapour deposition nano-diamonds on iridium. *New Journal of Physics*, 13(2):025012, February 2011.
- [15] S. A. Grudinkin, N. A. Feoktistov, A. V. Medvedev, K. V. Bogdanov, A. V. Baranov, A. Ya Vul’, and V. G. Golubev. Luminescent isolated diamond particles with controllably embedded silicon-vacancy colour centres. *Journal of Physics D: Applied Physics*, 45(6):062001, February 2012.
- [16] Elke Neu, Christian Hepp, Michael Hauschild, Stefan Gsell, Martin Fischer, Hadwig Sternschulte, Doris Steinmüller-Nethl, Matthias Schreck, and Christoph Becher. Low-temperature investigations of single silicon vacancy colour centres in diamond. *New Journal of Physics*, 15(4):043005, April 2013.
- [17] Jingyuan Linda Zhang, Hitoshi Ishiwata, Thomas M. Babinec, Marina Radulaski, Kai Müller, Konstantinos G. Lagoudakis, Constantin Dory, Jeremy Dahl, Robert Edgington, Veronique Soulière, Gabriel Ferro, Andrey A. Fokin, Peter R. Schreiner, Zhi-Xun Shen, Nicholas A. Melosh, and Jelena Vučković. Hybrid Group IV Nanophotonic Structures Incorporating Diamond Silicon-Vacancy Color Centers. *Nano Letters*, 16(1):212–217, January 2016.
- [18] Tina Müller, Christian Hepp, Benjamin Pingault, Elke Neu, Stefan Gsell, Matthias Schreck, Hadwig Sternschulte, Doris Steinmüller-Nethl, Christoph Becher, and Mete Atatüre. Optical signatures of silicon-vacancy spins in diamond. *Nature Communications*, 5:3328, February 2014.
- [19] Janine Riedrich-Möller, Carsten Arend, Christoph Pauly, Frank Mücklich, Martin Fischer, Stefan Gsell, Matthias Schreck, and Christoph Becher. Deterministic Coupling of a Single Silicon-Vacancy Color Center to a Photonic Crystal Cavity in Diamond. *Nano Letters*, 14(9):5281–5287, September 2014.
- [20] V. A. Davydov, A. V. Rakhmanina, S. G. Lyapin, I. D. Ilichev, K. N. Boldyrev, A. A. Shiryayev, and V. N. Agafonov. Production of nano- and microdiamonds with Si-V and N-V luminescent centers

- at high pressures in systems based on mixtures of hydrocarbon and fluorocarbon compounds. *JETP Letters*, 99(10):585–589, July 2014.
- [21] Andreas Dietrich, Kay D. Jahnke, Jan M. Binder, Tokuyuki Teraji, Junichi Isoya, Lachlan J. Rogers, and Fedor Jelezko. Isotopically varying spectral features of silicon-vacancy in diamond. *New Journal of Physics*, 16(11):113019, November 2014.
 - [22] Florian Böhm. *Low-Temperature Investigations of Silicon Vacancy Color Centers in Diamond Nanocrystals*. Master’s thesis, Ludwig-Maximilians Universität, München, 2015.
 - [23] C. D. Clark, H. Kanda, I. Kiflawi, and G. Sittas. Silicon defects in diamond. *Physical Review B*, 51(23):16681–16688, June 1995.
 - [24] Lachlan J. Rogers, Kay D. Jahnke, Marcus W. Doherty, Andreas Dietrich, Liam P. McGuinness, Christoph Müller, Tokuyuki Teraji, Hitoshi Sumiya, Junichi Isoya, Neil B. Manson, and Fedor Jelezko. Electronic structure of the negatively charged silicon-vacancy center in diamond. *Physical Review B*, 89(23):235101, June 2014.
 - [25] K.-M. C. Fu, C. Santori, P. E. Barclay, and R. G. Beausoleil. Conversion of neutral nitrogen-vacancy centers to negatively charged nitrogen-vacancy centers through selective oxidation. *Applied Physics Letters*, 96(12):121907, 2010.
 - [26] Elke Neu, Mario Agio, and Christoph Becher. Photophysics of single silicon vacancy centers in diamond: implications for single photon emission. *Optics Express*, 20(18):19956–19971, August 2012.
 - [27] C. Bradac, T. Gaebel, N. Naidoo, M. J. Sellars, J. Twamley, L. J. Brown, A. S. Barnard, T. Plakhotnik, A. V. Zvyagin, and J. R. Rabeau. Observation and control of blinking nitrogen-vacancy centres in discrete nanodiamonds. *Nature Nanotechnology*, 5(5):345–349, May 2010.
 - [28] Young-Shin Park, Andrew K. Cook, and Hailin Wang. Cavity QED with Diamond Nanocrystals and Silica Microspheres. *Nano Letters*, 6(9):2075–2079, September 2006.